Plasma Parameters and Weakly Non-Ideal Behaviour of a High Density, Super-Atmospheric 2 kA Cascade Arc in Argon

C. J. Timmermans, G. M. W. Kroesen, P. M. Vallinga, and D. C. Schram

Eindhoven University of Technology, Department of Physics, P.O. Box 513, 5600 MB Eindhoven, The Netherlands

Z. Naturforsch. **43 a,** 806–818 (1988); received April 30, 1988

Experimental results are reported for simultaneous pressure and current pulses up to 14 bar and 2200 A superimposed on an atmospheric pressure 60 A dc cascade arc. A current density over 10^8 A/m^2, previously 10^7 A/m^2 (power density 10^{12} W/m^3, previously 10^{10} W/m^3) has been obtained. The electron temperature of the thermal plasma was deduced from the end-on measured radiance of argon lines, and the electron density from the absolute continuum emission. The values found for the quantities mentioned during the quasi-stationary phase of the current pulse, lasting $\sim$1 ms, were 27 000 K and $3 \cdot 10^{23}$ m^{-3}, respectively, at a pressure of $\sim$1.5 bar (ionization degree 100%), and 18 000 K and $> 10^{24}$ m^{-3}, respectively, for a pressure of 14 bar (ionization degree 60%). These values satisfy the LTE relation. Deviations from the Spitzer conductivity have been observed in this weakly non-ideal plasma.

In general, the high ionized thermal plasma studied with its composition of neutral, singly ionized and doubly ionized argon atoms can serve as a useful medium for spectroscopic studies of highly ionized systems and as a valuable source of radiation in the visible a well as in the near and far ultraviolet parts of the spectrum.

Key words: High density, cascade arc, weakly non-ideal, super-atmospheric, argon.

I. Introduction

For the investigation of the properties of thermal plasma over a broad range of temperatures and electron densities it is necessary to generate a plasma under well defined conditions at predetermined values of current and gas pressure.

From a diagnostic point of view it is advantageous to use a cylindrical plasma column which is observed from an "end-on" position. Using this configuration an Abel conversion to construct the radial profiles of radiated emission is avoided. With the cascade arc, introduced by Maecker [1], both these requirements have been fulfilled in this work.

Many studies of the wall-stabilized plasma of this cascade arc were published; among others: [2–13]. Various gases and plasma conditions, mostly with pressures up to a few atmospheres and currents up to about 500 A were investigated.

Argon arc discharges in the pressure range up to 1000 bars and carrying currents up to 250 A were investigated by Bauder et al. [14, 15] with the purpose of studying non-ideal plasma behaviour.

This work deals with an argon cascade arc of 5 mm diameter and ca. 90 mm length with pressures up to 14 bars and current pulses up to 2200 A having a duration of $\sim$1 ms. These pressure and current pulses were superimposed on the so-called cw condition at atmospheric pressure carrying a 60 A DC.

The electron temperature has been determined by means of the source function method. The electron density has been calculated from the results of measurements of the absolute emission coefficient of continuous radiation. Both these points are described in Section II. Since the plasma in cw condition was treated in detail in [13, 16], we describe these items only briefly in Section III. Section IV starts with the experimental results for the case that only the argon pressure in the arc is pulsed. After that, results are given for the quasi-stationary phase appearing when pressure and current are pulsed simultaneously. The results include the electron temperatures, the attained electron densities and the electric field strength. Weakly non-ideality effects are noted. Section V is devoted to conclusions.

Reprint requests to Dr. C. J. Timmermans, Department of Physics, University of Technology, P.O. Box 513, Den Dolech 2, NL-5600 MB Eindhoven, The Netherlands.

0932-0784 / 88 / 0800-0806 $ 01.30/0. – Please order a reprint rather than making your own copy.

II. Determination of Electron Temperature and Electron Density from the Aquired Data

II.1. The Electron Temperature

The electron temperature has been determined with the source function method basically described in [17, 9, 13]. With this spectroscopic method radial profiles of spectral line emission and absorption have been obtained. Assuming PLTE, the radial profiles of the electron temperature can then be calculated from these data.

Electron temperature measurements for pulsed-arc conditions have been performed with a spectroscopic set-up similar to the one described in [13]. For these measurements the monochromator is adjusted to the top of a spectral line with the arc in the cw condition. If only the argon pressure was pulsed, the neutral-argon (ArI) line $\lambda_0 = 696.5$ nm was used, and when pressure and current were pulsed simultaneously the line $\lambda_0 = 480.6$ nm of singly ionized argon (ArII) was used. This 480.6 nm line is well separated from neighbouring lines [18, 19]. Control-measurements were carried out using the ArII lines $\lambda_0 = 473.6$ nm and $\lambda_0 = 488.0$ nm. For a given plasma condition no temperature difference were found that exceeded the error of measurement amounting to ca. 3%.

The transmittance width of the monochromator (ca. 0.04 nm) was much smaller than the spectral width of all spectral lines used and than the shift of the Stark broadened ArII line $\lambda_0 = 480.6$ nm [20–22].

II.2. The Electron Density

The electron density has been determined from the results of end-on measurements of the absolute value of the continuum radiance in the wavelength area around 468.8 nm (Figure 1). The width of the monochromator profile used was 0.16 nm. The wavelength area around 468.8 nm has been chosen for the mere reason that in this region there occur no argon atomic or ionic spectral lines, nor lines of possible impurities, viz. copper from the cascade plates or tungsten from the electrodes.

It turned out that the continuum emission coefficient is proportional to the electron density and in broad lines proportional to the ion density. Moreover, this emission coefficient depends weakly on the electron temperature. Therefore, if the electron temperature has been determined with an independent method as described in Subsect. II.1, and the ion densities have been expressed in the electron density, the absolute value of the continuum radiance serves as a very suitable and adequate diagnostic tool for the determination of the electron density.

The total spectral continuum emission coefficient ε_{tot} is described in [23] as

$$\varepsilon_{\text{tot}} = \varepsilon_{\text{ff}}^{\text{ei}} + \varepsilon_{\text{ff}}^{\text{ea}} + \varepsilon_{\text{fb}} \quad (\text{J/s m}^4\,\text{sr}). \tag{II.1}$$

The $\varepsilon_{\text{ff}}^{\text{ei}}$ and $\varepsilon_{\text{ff}}^{\text{ea}}$ are the free-free contributions of the electron-ion and the electron-neutral interactions, respectively; ε_{fb} represents the free-bound interactions. These terms can be written as follows:

$$\varepsilon_{\text{ff}}^{\text{ei}} = \sum_z \frac{C_1}{\lambda^2} \frac{n_e n_z}{\sqrt{T_e}} z^2 \exp\left[-\frac{hc}{\lambda k T_e}\right] \xi_{\text{ff}}(\lambda, T_e, z), \tag{II.2}$$

$$\varepsilon_{\text{ff}}^{\text{ea}} = \frac{C_2}{\lambda^2} n_a n_e T_e^{3/2} Q(T_e) \left\{\left(1 + \frac{hc}{\lambda k T_e}\right)^2 + 1\right\} \cdot \exp\left[-\frac{hc}{\lambda k T_e}\right], \tag{II.3}$$

and

$$\varepsilon_{\text{fb}} = \sum_z \frac{C_1}{\lambda^2} \frac{n_e n_z}{\sqrt{T_e}} z^2 \left\{1 - \exp\left[-\frac{hc}{\lambda k T_e}\right]\right\} \frac{g_{z,1}}{U_z} \xi_{\text{fb}}(\lambda, T_e, z), \tag{II.4}$$

where

$$C_1 = \frac{16\pi e^6}{3c^2(6\pi m_e^3 k)^{1/2}} \frac{1}{(4\pi\varepsilon_0)^3} = 1.6321 \cdot 10^{-43} \left(\frac{\text{J m}^4\,\text{K}^{1/2}}{\text{s sr}}\right),$$

$$C_2 = \frac{32 e^2}{3c^2} \left\{\frac{k}{2\pi m_e}\right\}^{3/2} \frac{1}{4\pi\varepsilon_0} = 1.026 \cdot 10^{-34} \left(\frac{\text{J m}^2}{\text{s K}^{3/2}\,\text{sr}}\right),$$

$\xi_{\text{ff}}(\lambda, T_e, z)$ Biberman factor for free-free radiation, including quantum, mechanical correction for non-hydrogenic atoms [23],

$\xi_{\text{fb}}(\lambda, T_e, z)$ Biberman factor for free-bound radiation, [24, 25],

n_e electron density (m^{-3}),

n_z z fold ionized density (m^{-3}),

z ion charge number $z = 1, 2$,

$g_{z,1}$ statistical weight of the ground level of the system Ar_z with charge z,

U_z partition function of Ar_z [26],

$Q(T_e)$ electron-neutral collision cross-section for momentum transfer integrated over the velocity distribution function (m^{-3}) [27],

λ, e, k, c and ε_0 have their usual meaning. For reasons of simplicity and clarity we omitted the subscript λ of the total spectral continuum emission coefficient and of all its spectral components.

In order to express the ion densities n_z of (II.2–4) as functions of the electron density n_e one has to take into account that with the rather extreme plasma conditions of pressures up to 14 bars and current up to 2200 A the plasma is highly ionized. We deal not only with argon neutrals (ArI) of density n_a and singly ionized argon ions (ArII) of density n_1, but also with doubly ionized argon ions (ArIII) of density n_2. Therefore, a summation including $z = 1$ and $z = 2$ in (II.2–4) is necessary.

Using the Saha relations, S_1 and S_2 that are functions of the electron temperature mainly, together with the quasi-neutrality conditions, n_a, n_1 and n_2 are found as functions of n_e and T_e. Substitution of these results into (II.2–4) leads to the total spectral continuum emission relation $\varepsilon_{tot}(\lambda, T_e, n_e^2, \xi)$. In this relation λ is the wavelength, n_e the electron density, T_e the electron temperature and ξ stands for the Biberman factors, appearing in the modified equation (II.1).

The Biberman factors for fb transitions to ArI and ArII are taken from Hofsaess [24, 25], those for ff transitions are calculated from Cabannes [23]. The fb transition from ArIV to ArIII may be neglected (see Fig. 2) and we only need to consider the transitions from ArIII to ArII and from ArII to ArI. Regarding i) the uncertainties in the Biberman factors, ii) the small differences between the actual electron density values and its LTE values, which will be verified later on and iii) the fact that by applying the Saha relations, equilibrium was already supposed, it is assumed to be justified to use this condition also in the expressions (II.1–4). It was already shown by solving the energy balance equation in [16] that in these pressure and current pulsed plasmas the deviations from equilibrium are rather small, i.e. less than 10%. In (II.1–4) these deviations have only a negligible influence. In this sense we can say that the effect of non-LTE is negligible in these equations.

Before discussing the calculation of the electron density in more detail, we want to evaluate the contributions of the separate continuum radiation processes

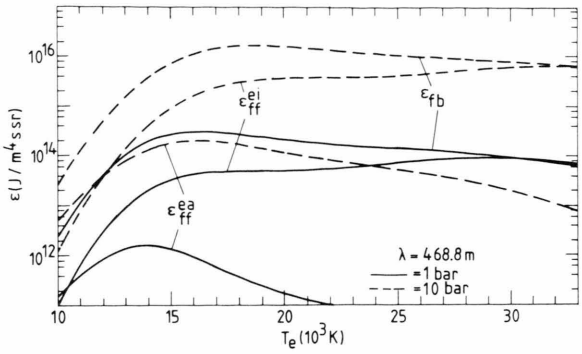

Fig. 1. Absolute values of the total spectral continuum emission coefficients ε_{fb}, ε^{ei}_{ff} and ε^{ea}_{ff} for $\lambda = 468.8$ nm vs. the temperature T_e, assuming LTE, for the pressures 1 and 10 bar.

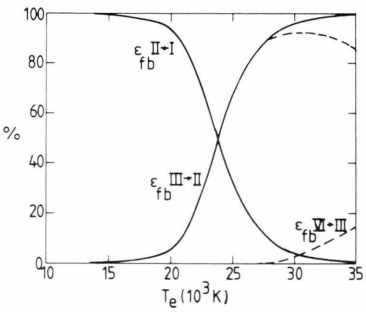

Fig. 2. Solid lines: the relative spectral contributions of ε^{II-I}_{fb} and $\varepsilon^{III-II}_{fb}$ to the total spectral ε_{fb} vs. the temperature T_e for the wavelength $\lambda = 468.8$ nm; higher transitions are excluded. Broken lines: including the contributions from $\varepsilon^{IV-III}_{fb}$.

to the total continuous radiation. One result of the application of (II.1–4) is that the continuum radiation of argon plasma in the range of temperatures and pressures studied is mainly produced by recombination processes (fb) between the electrons and the various kinds of ions present. In Fig. 1 the total spectral continuum emission coefficients for $\lambda = 468.8$ nm are given in absolute values as functions of the temperature for the pressures 1 and 10 bar, respectively. Other results are that the ff contribution originating from electron-ion interaction equals the fb contribution at about 30 000 K and that the ff contribution of electron-neutral interaction is less than 10% of the total radiation in the lower temperature range, see Figure 1.

Below a temperature of about 24 000 K the fb continuum almost completely originates from ArII to ArI transitions. This is illustrated in Fig. 2, where the separate relative fb contributions for ArII to ArI, for ArIII to ArII and also for ArIV to ArIII are given as func-

tions of the temperature. The transitions from ArIV to ArIII only come into play above about 28 000 K.

The end-on measurements yielded experimental absolute values of the spectral continuum radiance L_m of the plasma column. Here the subscript m is used to indicate the measured values; the wavelength indication λ is again omitted. This practice will be maintained in the following. From these experimental radiance values the absolute value of the total spectral continuum emission coefficient, $\varepsilon_{tot,m}$, is to be derived in order to calculate the electron density. In this calculation the reabsorption of the radiation over the plasma column length l_{pl} must be taken into account.

The measured spectral continuum radiance L_m, the total spectral continuum emission coefficient $\varepsilon_{tot,m}$ and the absorption coefficient $\varkappa$ are interrelated as follows:

$$L_m = \varepsilon_{tot,m} \int_0^{l_{pl}} \exp\{-\varkappa \cdot x\}\, dx$$

$$= \frac{\varepsilon_{tot,m}}{\varkappa} \{1 - \exp[-\varkappa \cdot l_{pl}]\}. \qquad \text{(II.5)}$$

Using Kirchhoff's law

$$\varepsilon_{tot,m} = \varkappa \cdot B(T_e)$$

and Planck's function

$$B(T_e) = \frac{2hc^2}{\lambda^5} \frac{1}{\exp\left[\frac{hc}{\lambda k T_e}\right] - 1}$$

one obtains

$$\varepsilon_{tot,m}\, l_{pl} = -B(T_e) \ln\left\{1 - \frac{L_m}{B(T_e)}\right\}. \qquad \text{(II.6)}$$

Using (II.6), the absolute value of $\varepsilon_{tot,m}$ is calculated from the measured value of L_m and the known value of $B(T_e)$, since T_e is known.

The overall conclusion is, that with known wavelength (λ), electron temperature (T_e), Biberman factors (ξ) and absolute value of the total spectral continuum emission ($\varepsilon_{tot,m}$), the electron density (n_e) can be calculated with the aid of a computer program, based on the modified equation (II.1), where n_e is an implicit parameter:

$$\varepsilon_{tot,m} \equiv \varepsilon_{tot}(\lambda, T_e, n_e^2, \xi). \qquad \text{(II.7)}$$

The uncertainty in l_{pl}, the length of the plasma column, amounts to about 2%. The absorption factor $\{1 - \exp[-\varkappa \cdot l_{pl}]\}$ ranges from a few percent in the low pressure arc up to about 90% in the arc at 14 bars pressure. This point will be discussed in Section IV.

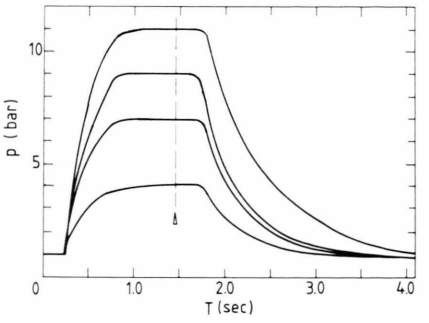

Fig. 3. Pressure pulses vs. time for four initial pressures in the high pressure argon reservoir. p = argon pressure in the arc chamber. The arrow indicates the timing of the current pulse; the pretrigger time is slightly less than 1.5 s.

The correction Δp on Dalton's law is taken from Griem [28] as

$$\Delta p = -\frac{1}{6} \frac{e^2}{4\pi\varepsilon_0} \frac{n_e + \sum_i z_i n_i}{\lambda_D}. \qquad \text{(II.8)}$$

where λ_D is the Debye shielding length including the influence of the ions. Although this pressure correction is almost negligible ($\sim$1.4%), it is taken into account in the calculation of the electron density. The correction for the lowering of the ionization potentials is duly applied in the Saha relations [26].

It follows from the obtained values of the density that the ionization degree of the plasma we studied is very high, viz. 60–100%.

III. Experimental Set-Up and Data Aquisition System

The cascade arc construction and the spectroscopic set-up used were extensively described in the literature. We refer to [9, 13, 16] for information on these items.

In order to generate a pressure pulse, the gas chamber of the cascade arc was connected to a high pressure argon gas reservoir. The gas pressure in the arc chamber was measured by means of a vibration-compensated piezo element in combination with a charge amplifier (Fa. Kistler, types 601 A and 501).

Figure 3 gives the argon pressure in the chamber as a function of time. Each time a nearly constant value of the gas density is obtained having a duration of

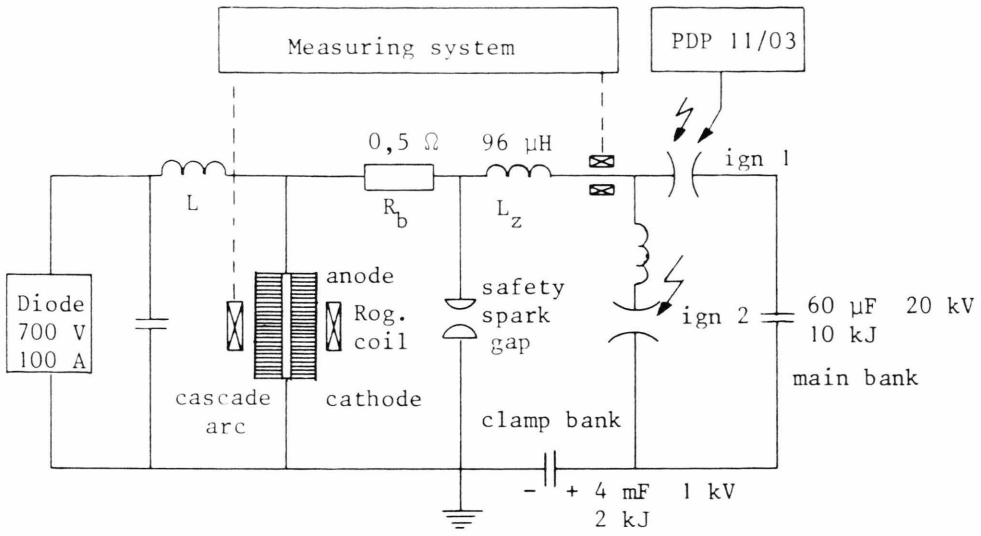

Fig. 4. Basic electric diagram of the DC power supply and the capacitor device both connected to the cascade arc.

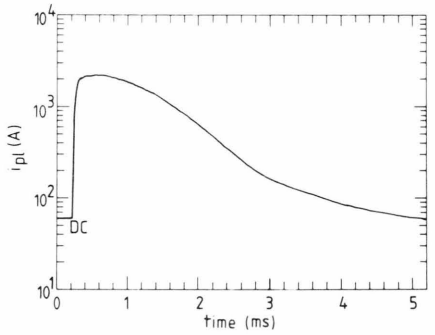

Fig. 5. The profile of the current pulse superimposed on the 60 A DC stationary arc vs. time, i_{pl} is the plasma current.

about 1 s. This time is very long as compared to the times associated with the electronic phenomena in the arc. Accordingly, the arc is in a steady regime during this plateau of the pressure pulse.

If, during a pressure pulse, a current pulse was applied, a capacitor bank was connected to the cascade arc by means of a trigger pulse. This trigger pulse was applied some time after connecting the arc chamber to the high pressure reservoir. This time, called the pretrigger time was adjusted with the aid of a DEC PDP 11/03 computer in such a way that the current pulse arrived during the steady regime of the arc at about two-thirds of the pressure plateau.

The basic diagram of the electric circuit is shown in Figure 4. In this diagram there are two capacitors and two ignitrons. Ignitron 1 is triggered by the computer controlled trigger pulse. The 60 μF capacitor is inserted in series with the 4 mF capacitor, the 96 μH induction coil (L_z) and the total ohmic resistance of the load resistor R_b and the cascade arc. A current rise sets in up to ~2200 A within about 60 μs. At the maximum of this current pulse ignitron 2 is triggered, also by the DEC PDP 11/03 computer and the 4 mF capacitor bank, the clamp bank takes over, lengthening the duration of the current pulse. The quasi-stationary phase of the current pulse is roughly 1 ms, see Figure 5. The plasma current was measured with a Rogovski coil surrounding the arc itself.

The plasma ohmic resistance depends on gas pressure and electron temperature, consequently it varies over a range of about 0.3 Ω with various experimental conditions. This variation cannot be neglected with respect to the load resistor R_b of 0.5 Ω, cf. Figure 4, and thus it influences the shape of the current pulse. By variation of the voltages impressed on each of the capacitor banks the currernt profiles were corrected to maintain the same shape for all the experimental conditions.

The safety spark gap is necessary to avoid damage of the arc construction itself if during a shot the plasma current is unexpectedly interrupted.

The electric field strength follows from the measurement of the potential drop between two plates of the cascade arc chamber serving as measuring probes. These plates were located with an accurately known distance between them. Also they were placed four to

five times the arc diameter from the electrodes in order to avoid end effects and electrodes effects.

The signals representing the spectral intensities, the pressure pulses, the plasma current pulses and the electric field strengths were stored in transient recorders having a sampling time of 5 μs. These measured data could be read by the PDP 11/03 and were sent to and stored in a DEC PDP 11/23 computer, which serves as a file handler. The accumulated data of many shots were sent from the PDP 11/23 to the central Burroughs B 7900 computer of the University, where they were permanently stored. With the aid of software developed for the B 7900 the plasma quantities were calculated from the acquired data.

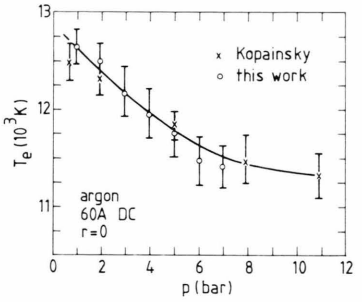

Fig. 6. The electron temperature T_e in the central region of the arc ($r=0$) vs. the pressure p for a 60 A DC cascade arc, $\times\times$: [3]. oo: this work. Vertical bars are the error bars for 95% reliability.

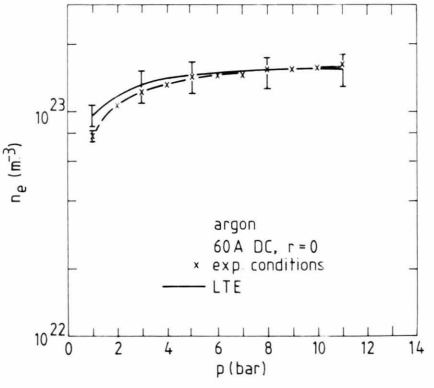

Fig. 7. Electron density n_e vs. the argon pressure p for the central region of the 60 A DC cascade arc. $\times\times$: electron densities determined from the continuum emission and the corresponding values of the electron temperature on the curve of Fig. 6; solid line: electron density calculated under assumption of LTE from the gas pressure p and the corresponding electron temperature on the curve of Figure 6.

IV. Experimental Results and Discussions

IV.1. Results for the Experiments in which Only the Argon Pressure is Pulsed

In these experiments the plateau pressure varied from 1 bar to 11 bar, the arc current was always 60 A.

The source function method, applied for the determination of the electron temperatures, has optimum accuracy if the spectral line used shows significant absorption in the line of sight of the monochromator. The optical depth $\varkappa l$ ($l=90$ mm) should preferably surpass the value 0.3. When only the pressure was pulsed in the cascade arc, this condition was satisfied for the ArI line $\lambda=696.5$ nm used for these experiments. It was not satisfied for the ArII line $\lambda=480.6$ nm that has been used when the current was pulsed as well as the pressure (see Subsection IV.2).

Figure 6 gives the electron temperature in the central region of the arc as a function of the gas pressure together with the values obtained by Kopainsky from measurements in a similar arc [3]. There is good agreement between the two sets of measurements.

The electron density in the central region of the arc as calculated from the measured absolute value of the continuum emisssion is given in Fig. 7 as a function of the measured gas pressure. The measured continuum intensity values have been corrected for the absorption over the arc length. This absorption increases from about 1% for the arc at 1 bar up to about 6% at 11 bar gas pressure.

The solid line in Fig. 7 gives values of the electron density, calculated from the LTE model, using the measured pressures and the corresponding temperatures of the experimental curve of Fig. 6. The error bars represent possible variations (95% reliability) in the electron densities due to uncertainties in the quantities underlying the calculation.

From Fig. 7 the conclusion may be drawn that for pressures of 2 bar and more the pressure pulsed cascade arc is very close to LTE. The deviation at 1 bar is in agreement with the non-equilibrium effects found in [9, 13].

According to Fig. 3 the duration of the pressure plateau is about 1 s for all pressures up to 11 bar. During this plateau the arc may be assumed to be in a stationary state. This statement is in agreement with the stability criterion formulated by Bauder [15] for 5 mm diameter cascade arc chambers with plates of

≈2 mm thickness. Bauder investigated cascade arcs up to 300 bar at currents up to 250 A in argon. At low gas pressures and high currents the arc became unstable as a consequence of arcing between neighbouring plates, caused by exceedingly high electric field strengths (about 7500 V/m) between the plates. When in our experiment only the argon pressure was pulsed, the field strength remained always far below this stability limit. The highest values registered were about 1500 V/m.

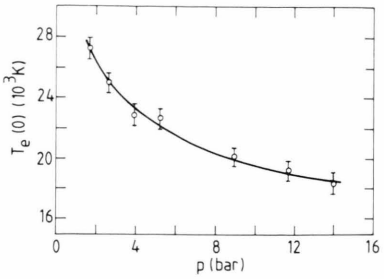

Fig. 8. The electron temperature T_e in the arc centre for the quasi-stationary phase of the current pulse ($I \approx 2200$ A) vs. the argon pressure p.

IV.2. Results for the Cascade Arc with Simultaneous Pulsed Pressure and Current

In this mode of operation of the cascade arc at a pressure about 1.65 bar an electric field strength of about 8000 V/m is measured, see Figure 14. This value touches the range, where Bauder [15] stated that arcing between the plates may occur. Therefore special attention was paid to oscillations in electron temperature and density observed at the very beginning of the quasi-stationary phase of the current pulse. These oscillations were found to be opposite in phase with the electric field strength oscillations that were observed as well. In the arc current no oscillations were noticed. In combination with Ohm's law these findings imply that the oscillations we came across are due to pressure variations and not to arcing between the cascade plates. For pressures exceeding 1.65 bar the electric field strengths were found to be less than 8000 V/m, see Figure 14.

The Electron Temperature Results

With simultaneously pulsed pressure and current in the cascade arc the source function method has been applied to the ArII line 480.6 nm for the determination of the electron temperature. In the current pulsed cascade arc this line is absorbed strongly enough to satisfy the condition $\varkappa l > 0.3$ (with $l = 90$ mm) for optimum accuracy of the method. During the 60 μs risetime of the current pulse the optical depth for the ArII line increases rapidly and reaches a value in the neighbourhood of $\varkappa l = 4$. The consequence is that in end-on observation the ArII line is strongly absorbed in its central wavelength $\lambda = 480.6$ nm and that here its radiance approaches that of the Planck radiator of temperature T_e. Beyond the quasi-stationary phase the arc current decreases relatively slowly to its DC value, viz. 60 A, see Figure 5. Roughly 2 ms after the trigger pulse the current is about 600 A and the optical depth of the arc has decreased to ca. 0.3. Later on in the pulse at still lower currents the source function method is no longer applicable with any accuracy.

In Fig. 8 the electron temperature in the central arc region is given as a function of the gas pressure prevailing in the quasi-stationary phase of the current pulse. For all studied pressures the measured radial electron temperature distributions show a rather flat profile up to the reduced radius $r/R \approx 0.7$; the arc chamber radius $R = 2.5$ mm [16].

The Electron Density Results

The electron density in the quasi-stationary phase of the current pulse ($I = 2200$ A) has been determined from the measured values of the continuum radiance in the vicinity of the wavelength 468.8 nm. In Fig. 9 the results of these determinations for the arc centre are plotted against the plateau pressure p of the underlying pressure pulse. The electron temperatures found in these experiments are given as annexes to the crosses representing the electron densities. In the same figure the broken line represents the electron density $n_{e,\mathrm{LTE}}$, calculated for LTE conditions, as a function of the gas pressure. The starting points of this calculation for a given pressure (chosen from the values occuring in the experiments) were the electron temperature taken from the experimental curve of Figure 8, the Saha relations, Dalton's law and the quasi-neutrality condition. Two corrections were taken into account: viz. the decrease in ionization potential according to Debye-Hückel [26] and the correction of Dalton's law for dense plasmas [28].

From Fig. 9 it may be concluded that in the quasi-stationary phase of the current pulse with a current of

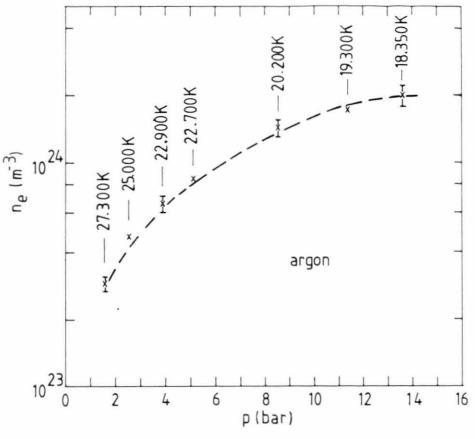

Fig. 9. The electron density n_e in the quasi-stationary phase of the current pulse ($I \approx 2200$ A) for central arc domain vs. the plateau pressure p of the pressure pulse. The broken curve represents the $n_{e,\,LTE}$ value. Indicated are the measured temperatures at the same plasma conditions and radial position also for the central arc domain.

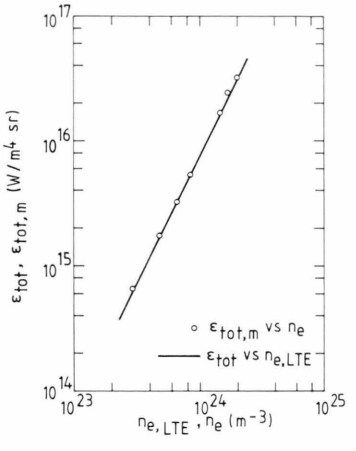

Fig. 10. Solid line: the theoretical absolute spectral continuum emission coefficient ε_{tot} as calculated under LTE conditions vs. the LTE value $n_{e,\,LTE}$ of the electron density. Circles: Experimental values of the electron density n_e (on the horizontal axis) following from the measured absolute value of the spectral total continuum emission coefficient $\varepsilon_{tot,\,m}$.

ca. 2200 A and in the range of electron densities of $3 \cdot 10^{23}\,m^{-3}$ to ca. $2 \cdot 10^{24}\,m^{-3}$ the plasma is in or very close to LTE.

Experimental radial electron density profiles are rather flat up to the reduced radius of $r/R \approx 0.7$ (with $R = 2.5$ mm) over the whole pressure range [16].

From (II.1) and with the gas pressure, the corresponding experimental value of the electron temperature and the electron density under LTE conditions ($n_{e,\,LTE}$), the theoretical value of the spectral continuum emission coefficient (ε_{tot}) was calculated. The result is shown in the solid line of Fig. 10 as a function of $n_{e,\,LTE}$.

The reasoning may also be made the other way around: the circles in Fig. 10 represent experimental values of the electron density (n_e now plotted on the horizontal axis) versus the measured values $\varepsilon_{tot,\,m}$ of the total spectral emission coefficient (on the vertical axis).

The conclusion from Fig. 10 is the same as that from Figure 9. The plasma studied is in or very close to LTE.

Under the realized conditions the ionization degree of the plasma is between 100% at 1.65 bar argon pressure and 60% at 14 bar pressure, cf. Figure 12. Further it is evident from Fig. 9 that the electron and ion densities in these plasmas reach up to values beyond $10^{24}\,m^{-3}$. In these situation the plasmas are good media for the study of non-ideality effects. These effects will be discussed in Subsection IV.3.

A Remark with Regard to the Biberman Factors

Many reports of investigations relating to the Biberman factors we applied, are found in the literature, among others [19, 24, 29–31]. Biberman factors appear as linear components in the expression for the emission coefficient, cf. (II.2–4). Large uncertainties in these factors spoil the reliability of the interpretation considerably.

In the present work the electron density for the quasi-stationary phase of the current pulse at a pressure of 1.65 bar has been determined in two ways: The method based on the measurement of the continuum radiation emission was applied as usually in this work, and moreover a method was used based on feed-back interferometry [13, 16]. In the former method the Biberman factors as calculated by [24, 25] were used and the electron density $(2.9 \pm 0.2) \cdot 10^{23}\,m^{-3}$ was found, see Figure 9. In very good agreement with this result the latter method yielded the value $(2.7 \pm 0.3) \cdot 10^{23}\,m^{-3}$.

As this comparison between the continuum radiation method and the interferometric method was made for several temperatures from 12 700 up to 27 000 K, the conclusion may be drawn that Hofsaess' Biberman factors for the transition from ArII to ArI

are reliable in this range of temperatures. Besides this, we point out that these values are within 10% of those obtained by other authors [29–31]. Consequently we assumed that the factors as calculated by Hofsaess for the transition from ArIII to ArII may be used with confidence as well, so that we applied his Biberman factors for the whole range of temperatures of this study.

Remarks with Regard to the Absorption Continuum Radiation

For current densities smaller than roughly 10^7 A/m^2 cascade arcs described in the literature show only a few percents reabsoption of visible continuum radiation. For comparison with the results of this work a brief survey of the results of some experiments will be given in the following.

Self-absorption of continuum radiation increases with increasing gas presssure, arc length, current density (power density) and wavelength. Therefore the most extreme conditions with respect to the phenomenon of interest have the highest values for the variables mentioned. As the arc lengths used in the various experiments are not essentially different from our value ($l_{pl} = 90$ mm), this variable will be left out of consideration.

Lee et al. [4] studied an argon cascade arc with pressures up to 10 bar and current densities up to about 10^7 A/m^2 (power density up to $2 \cdot 10^{10}$ W/m^3) in the wavelength interval of 80–3860 nm. Even under their most extreme conditions ($\lambda = 3.86$ μm, $I = 400$ A, $p = 10$ bar) the self-absorption appeared to be less than 1%.

Preston [32] reported on a 3 mm diameter wall-stabilized argon plasma at pressures of about 2 bar and current densities up to about 10^7 A/m^2 (power density up to 10^8 W/m^3). In the wavelength interval of 120–340 nm the absorption effects along the arc were less than 1.5%.

Goldbach et al. [19] reported on argon continuum measurements for a 5 mm diameter cascade arc with pressures up to 30 bar. With a current density of about 10^7 A/m^2 (power densities ca. $2 \cdot 10^{10}$ W/m^3, axis temperature of 11 200 K), the self-absorption at the wavelength $\lambda = 447.0$ nm amounted to 11% in the extreme case.

It is woth noting here that in the present work in the pressure range 1–14 bar a current density over

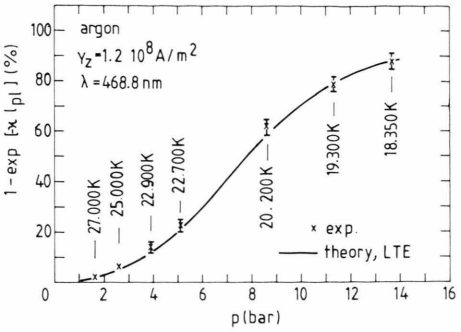

Fig. 11. Absorptance $1-\exp(-\varkappa l_{pl})$ in the vicinity of $\lambda = 468.8$ nm vs. the pressure p. – × ×: are the experimental points. The corresponding temperatures on the arc axis are indicated as annexes to the crosses, the broken line is the theoretical curve.

10^8 A/m^2 (power density about 10^{12} W/m^3) was achieved in the temperature range from 18 000 K to 27 000 K. This is quite an extended domain of plasma variables as compared to the ones cited.

The absorptance α_{lm} over the plasma length l_{pl} can be calculated from the measured absolute spectral continuum radiance L_m as follows (see (II.5)):

$$\alpha_{lm} = 1 - \exp[-\varkappa(\lambda)\, l_{lp}] = \frac{L_m}{B(T_e)}. \qquad \text{(IV.1)}$$

In this equation the value of Planck's function $B(T_e)$ is known as T_e has been determined in an independent way.

In Fig. 11 experimental values of the absorptance are plotted as crosses against the argon pressure. The corresponding temperatures on the arc axis are indicated as annexes of these crosses.

The theoretical value of the absorptance can be determined with the aid of the modified equation (II.1) from the LTE-value of the electron density and Kirchhoff's law. The broken line in Fig. 11 shows the result as a function of the gas pressure. The agreement between theory and experiment is quite satisfactory.

A rather strong increase of the absorptance up to roughly 90% at 14 bar pressure is evident. This fact indicates that at this pressure and along the line of sight in the central region of the arc having a length of ~90 mm, the plasma approaches the Planck limit. It can be considered to be nearly a black body radiator in the investigated continuum wavelength in the vicinity of $\lambda = 468.8$ nm.

IV.3. Electric Field Strength Measurements and Non-ideality Effects

The electrical conductivity is a suitable quantity to study non-ideality effects in dense plasmas. In most of the experimental investigations of non-ideality effects by means of the determination of the electrical conductivity, a problem arises since most are only partially ionized. Hence, additional theoretical difficulties come up owing to the influence of the neutral particles since non-ideality effects must be separated from the effect of electron-neutral collisions.

Therefore, the study of the non-identity of dense plasmas it is desirable that the degree of ionization be as high as possible and at least so large that electron-ion encounters dominate by far the influence of electron-atom collisions.

Non-ideality studies based on measurements of the electrical conductivity in partially ionized gases were performed by several authors. Bauder and Devoto [14, 15, 33] investigated these effects in a cascade arc for pressures up to 300 bar and currents up to 150 A, obtaining current densities of about $8 \cdot 10^6$ A/m^2. Goldbach et al. [34] studied cascade arcs up to 175 A in the pressure range of 1–20 bar with a current density of about $9 \cdot 10^6$ A/m^2. Günther et al. [35] reported on the electrical conductivity in a weakly non-ideal current pulsed argon plasma generated in a quartz tube at pressures up to 20 bar and with a pulsed current of about 2 kA, obtaining a current density of about $4 \cdot 10^7$ A/m^2.

In this work the non-ideality effect has been studied in the cascade arc with pressures up to 14 bar and with a pulsed current of about 2200 A with current densities over 10^8 A/m^2. In most cascade arcs (normally operating with stationary currents of 60 to 250 A), the ionization degree reaches a maximum of about 70% for an argon pressures of 1 bar and decreases with increasing pressure, see Figure 12. The ionization degree is defined as $\alpha = n_e/(n_e + n_a)$, where n_a the neutral density.

This figure shows also that in the current pulsed plasma the degree of ionization approaches 100% at 1 bar pressure and is still as high as 60% for a pressure of 14 bar.

It can be deduced from Fig. 13 that the electron-neutral interactions play only a minor role in relation to the electron-ion encounters in the highly ionized plasma we studied. The ratio of the conductivity of partially ionized gases (σ_F) to that of fully ionized gases (σ_{Sp}) is platted as a function of the temperature in this figure for three gas pressures.

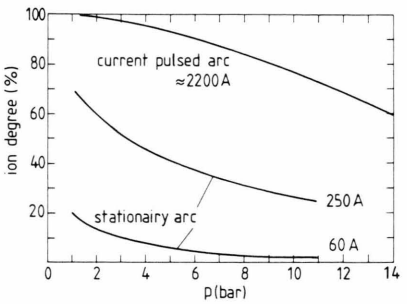

Fig. 12. Degree of ionization (%) vs. the gas pressure p for the 2200 A current pulsed arc and for stationary arcs with 60 A and 250 A currents.

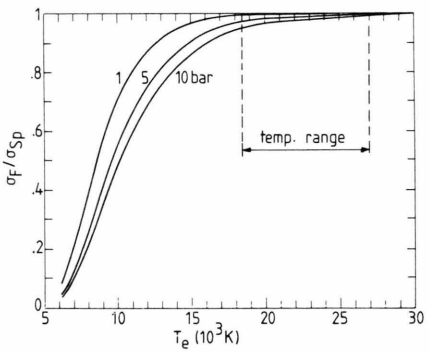

Fig. 13. The ratio σ_F to σ_{Sp} as a function of temperature T_e with the pressure $p = 1$, 5 and 10 bar as parameter. "temp. range" = temperature range covered by our experiments.

The conductivity of a partially ionized gas (σ_F) is derived with the aid of the mixture rule of Frost [36], which takes into account the electron-neutral interactions. This rule is known to represent the measured conductivities in the whole range of weakly to fully ionized plasmas very well.

The electrical conductivity for fully ionized gases (σ_{Sp}) is taken from Spitzer et al. [37] and is based on the Debye shielding model, viz.

$$\sigma_{Sp} = \frac{n_e e^2}{m_e \nu_{ei}} = \frac{32\sqrt{\pi}\,\varepsilon_0^2 (2kT_e)^{3/2}}{e^2 \sqrt{m_e}\,\langle Z\rangle \ln \Lambda}\,\gamma_E\,. \qquad \text{(IV.2)}$$

where ν_{ei} is the electron-ion collision frequency as defined in [38], $\langle Z\rangle = (1 + \sum z_i^2 n_i/n_e)$ and γ_E stands for the electron-electron interactions. Note that in the definition of the Debye shielding length (λ_D) the influence of the ions is taken into account as defined in [28], viz.

$$\lambda_D = \left\{ \frac{\varepsilon_0 k T_e}{e^2 (n_e + \sum z_i^2 n_i)} \right\}^{1/2}. \qquad \text{(IV.3)}$$

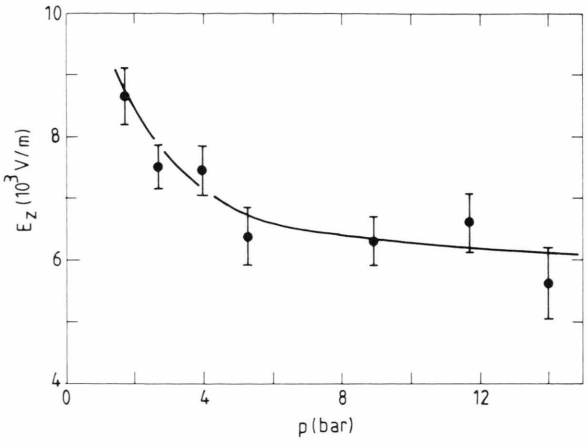

Fig. 14. The measured electric field strength E_z vs. the pressure p in the quasi-stationary phase of the current pulse.

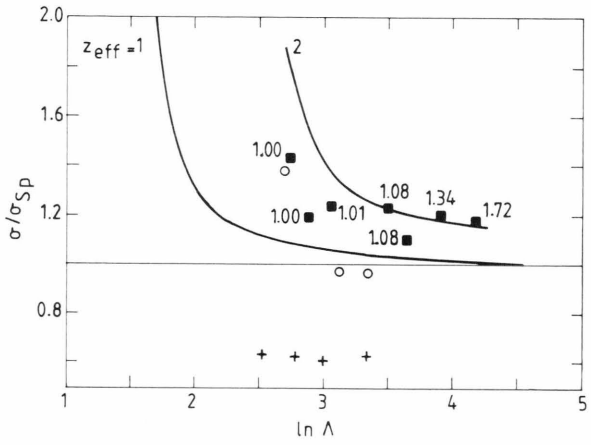

Fig. 15. The electric conductivity (σ) of weakly non-ideal plasmas normalized to Spitzer conductivity (σ_{Sp}) vs. the Coulomb logarithm ($\ln \Lambda$). – Full lines are the theoretical values [40–42] for ionic charge $Z_{eff}=1$ and $Z_{eff}=2$. – □□: Experimental points from this work, Z_{eff} values given as annexes to these points; ○○: experimental points from [15] and ++ from [35].

In the Coulomb logarithm $\ln \Lambda = \ln \lambda_D / b_0$, b_0 is the minimum impact parameter defined as $b_0 = e^2/(4\pi\varepsilon_0 3kT_e)$. The value of σ_{Sp} depends predominantly on the electron temperature and, via the Coulomb logarithm, weakly on the electron and ion density.

It is evident from Fig. 13 that for the temperature range in our experiments in the quasi-stationary phase the current pulse σ_F is nearly equal to σ_{Sp}. Therefore we normalized the measured conductivity with σ_{Sp}, a procedure commonly followed in the literature [33, 35].

The electrical conductivity $\sigma(T)$, the current density j and the electric field strength E are interrelated through Ohm's law $j = \sigma E$. The magnitude of the electric field strength E_z, measured as described in Sect. III, is shown in Fig. 14 for the quasi-stationary phase of the current pulse as a function of the pressure.

The electric field strength is assumed to be radially independent as a consequence of $\nabla \times \boldsymbol{E} = -\mathrm{d}\boldsymbol{B}/\mathrm{d}t \approx \boldsymbol{0}$ and of the axial homogeneity of the arc. This was experimentally verified by Uhlenbusch et al. [39], who measured the radial potential distribution in cascade arcs.

The axial current density j_z is calculated from the measured current in the pulse. As discussed in [16], [6], the axial current density shows a very flat profile nearly up to the wall. Therefore we assume the effective area for the current to be πR^2, and the current density is calculated as $j_z = I/\pi R^2$, where R is the full arc channel radius, viz. $2.5 \cdot 10^{-3}$ m. This is of course a slight underestimate of the axial current density, and therefore we obtain also a slight underestimate of the electric conductivity as calculated from Ohm's law $\sigma_{meas} = j_z/E_z$. The error involved is estimated to be about 6%.

A presentation of the measured non-ideality effect is given in Fig. 15, where the measured electrical conductivity (σ_{meas}), normalized to the Spitzer conductivity (σ_{Sp}), is given as a function of the Coulomb logarithm ($\ln \Lambda$). Some other experimental data obtained from argon arc discharges [15, 33, 35] are also shown.

Brouwer et al. [40, 41] have solved the kinetic equation for a fully ionized plasma in the situation that the frequency of the external electric field is much smaller than the electron plasma frequency. Calculating the electric conductivity on this basis, Brouwer found good agreement with results reported previously by Williams et al. [42] for the DC case. In Fig. 15 the solid lines represent Brouwer's theoretical calculations, normalized to Spitzer's value, as a function of the Coulomb logarithm for two values of the ionic charge parameter $Z_{eff} = \sum z_i^2 n_i/n_e$, viz. 1 and 2. As annexes to our experimental points the corresponding Z_{eff} values are given in Figure 15.

Differences between the experimental results may partially be explained by differences in plasma characteristics and in experimental devices. In the experiments of Bauder [15, 33] and of Günther et al. [35] the temperatures varied in the interval 10 000–15 000 K, whereas in this study the interval was 18 000–27 000 K. This means that there is a difference in the degree of ionization which may be decisive for the question as to whether the plasma may by treated as fully ionized or

not. As to the experimental devices, the difference lies in the fact that Bauder's experiments and this study were performed in cascade arcs while Günther's experiments took place in quartz flash tubes.

Although the cascade arc experimental points are situated near or between the theoretical curves, the available experimental work leads to the conclusion that the problem as to whether the electrical conductivity increases or decreases by non-ideality effects is not solved as yet.

Nevertheless, the effect of weakly non-ideality is evident in the argon plasmas we studied.

V. Concluding Remarks

A current pulse of 2200 A having a duration of about 1 ms can be superimposed on the DC current of a pressure pulsed cascade arc without causing arcing between the cascade plates. In this way the usual power density of a few times 10^{10} W/m^3 under stationary arc conditions is extended to about 10^{12} W/m^3. In the literature, cascade arc experiments with current densities of about 10^7 A/m^2 were described; in the present work this current density range has been extended to values exceeding 10^8 A/m^2.

During the quasi-stationary phase of the current pulse at a pressure of about 1.5 bar an electron temperature of 27 000 K and an electron density of $3 \cdot 10^{23}$ m^{-3} have been obtained; while at a pressure of 14 bar a temperature of 18 000 K and an electron densities over 10^{24} m^{-3} have been observed.

The electron temperature of the plasma in the quasi-stationary phase of the pulsed arc was deduced from the end-on measured spectral radiance of the ArII $\lambda =$ 480.6 nm line. Over the whole pressure range the optical depth of this line is sufficiently large (i.e. $\varkappa l > 4$), so that the spectral radiance of the line approaches Planck's limit.

The absorption of the visible continuum radiance over the length of the arc range from a few percent in the lower pressure range to nearly 90% for the 14 bar plasma. This implies that even the visible continuum radiation of the pulsed arc approaches the Planck limit.

Electron densities derived from the absolute continuum emission and the electron temperature satisfy the LTE relation during the quasi-stationary phase of the arc.

The pulsed arc plasma, which is found to be 100% ionized at 1.5 bar pressure and 60% ionized at 14 bar, is appropriate to the study of non-ideality effects in plasmas.

Generally spoken, the thermal plasma studied with its composition of neutral argon atoms, as well as singly and doubly ionized charged argon ions is very close to LTE. Therefore it can serve as a suitable medium for spectroscopic studies of highly ionized systems. It is a valuable source of radiation in the visible as well as in the near and far ultraviolet parts of the spectrum. Finally, it can be used for the study of e.g. transport properties, transmission probabilities of highly ionized ions and Stark effects under these conditions.

Acknowledgements

The authors are indebted to Mr. G. Hermkens and Dr. Z. Kolacinski for their fruitful cooperation and for many valuable discussions relating to this work. They also acknowledge the skillful technical assistance of Mr. J. J. Bleize and Mr. L. A. Bisschops. To Mr. A. B. M. Hüsken they are thankful for his indispensable assistance with electronics. Further the authors appreciate the assistance of Mr. P. van Haren with the temperature measurements of the pressure pulsed arc. Finally they wish to express their gratitude to Prof. Dr. A. A. Kruithof and Dr. H. H. Brouwer for the support in reading the manuscript and for the advices with regard to the article.

[1] H. Maecker, Z. Naturforsch. **11a,** 457 (1956).
[2] J. F. Uhlenbusch and E. Fisher, Proc. IEEE **59,** 578 (1971).
[3] J. Kopainsky, Z. Phys. **248,** 417 (1971).
[4] J. B. Lee and F. P. Incropera, J. Quant. Spectrosc. Radiat. Transfer **13,** 1539 (1973).
[5] J. Leclair and D. C. Schram, Proc. XIIIth ICPIG, Berlin 1977, p. 483.
[6] R. J. Rosado, J. Leclair, and D. C. Schram, Proc. XIIIth ICPIG, Berlin 1977, p. 573.
[7] H. Kafrouni, J. M. Bageaux, A. Gleizes, and S. Vacquie, J. Quant. Spectrosc. Radiat. Transfer **21,** 457 (1979).
[8] V. Helbig and K. P. Nick, J. Phys. B: At. Mol. Phys. **14,** 3573 (1981).
[9] R. J. Rosado, An investigation of non-equilibrium effects in thermal argon plasmas, Ph.D. thesis, Eindhoven University of Technology, Eindhoven, The Netherlands, 1981.
[10] R. J. Rosado, C. J. Timmermans, D. C. Schram, and V. Hellbig, Proc. XVth ICPIG, 1249 Minsk (1981).
[11] K. P. Nick, Analyse des Plasmazustandes und Bestimmung atomarer Konstanten in einem Argon-Kaskadenbogen, Ph.D. thesis, University of Kiel, BRD 1982.

[12] A. Gleizes, H. Kafroni, H. Dang Duc, and C. Maury, J. Phys. D: Appl. Phys. **15,** 1031 (1982).
[13] C. J. Timmermans, R. J. Rosado, and D. C. Schram, Z. Naturforsch. **40a,** 810 (1985).
[14] U. H. Bauder and E. D. Stephan, Rev. Sci. Instrum. **43,** 1341 (1972).
[15] U. H. Bauder, Appl. Phys. **9,** 105 (1976).
[16] C. J. Timmermans, An investigation of pulsed high density plasmas, Ph.D. thesis, Eindhoven University of Technology, Eindhoven, The Netherlands, 1984.
[17] H. W. Drawin, Phys. Lett. **42A,** 423 (1973).
[18] R. C. Preston, J. Quant. Spectrosc. Radiat. Transfer **18,** 337 (1977).
[19] C. Goldbach, G. Nollez, and P. Plomdeur, J. Phys. B: Molec. Phys. **10,** 1181 (1977).
[20] G. A. J. Hermkens, Private communication, intern report, University of Technology, Eindhoven, The Netherlands, Department of Physics, VDF/NT-82-9, 1982.
[21] G. M. W. Kroesen, Private communication, intern report, University of Technology, Eindhoven, The Netherlands, Department of Physics, VDF/NT-83-07, 1983.
[22] H. W. Drawin, Z. Phys. **225,** 470 (1969).
[23] F. Cabannes and J. C. Chapelle, in: Reactions under Plasma Conditions, ed. M. Venugopalan, John Wiley & Sons, New York 1971.
[24] D. Hofsaess, J. Quant. Spectrosc. Radiat. Transfer **19,** 339 (1978).
[25] D. Hofsaess, Private communication, 1982.
[26] H. W. Drawin and P. Felenbok, Data for Plasmas in Local Thermodynamic Equilibrium, Gauthier-Villars, Paris 1965.
[27] R. S. Devoto, Phys. Fluids **16,** 616 (1973).
[28] H. R. Griem, Phys. Rev. **128,** 997 (1962).
[29] E. Schulz-Gulde, Z. Phys. **230,** 449 (1970).
[30] D. Meiners and C. O. Weiss, J. Quant. Spectrosc. Radiat. Transfer **16,** 273 (1976).
[31] S. E. Schneehage, M. Kock, and E. Schulz-Gulde, J. Phys. B: Atom. Molec. Phys. **15,** 1131 (1982).
[32] R. C. Preston, J. Phys. B: Atom. Molec. Phys. **8,** 1573 (1977).
[33] U. H. Bauder, R. S. Devoto, and D. Mukherjee, Phys. Fluids **16,** 2143 (1973).
[34] C. Goldbach, G. Nollez, S. S. Popovic, and M. M. Popovic, Z. Naturforsch. **33a,** 11 (1978).
[35] K. Günther, S. Lang, and R. Radtke, J. Phys. D: Appl. Phys. **16,** 1235 (1983).
[36] L. S. Frost, J. Appl. Phys. **32,** 2029 (1961).
[37] L. Spitzer and R. Härm, Phys. Rev. **89** (5), 977 (1953).
[38] M. Mitchner and C. H, Kruger, Partially Ionized Gases, John Wiley and Sons, New York 1973.
[39] J. F. Uhlenbusch and G. Gieres, Z. Angew. Phys. **27,** 66 (1969).
[40] H. H. Brouwer, Kinetic theory of slightly non-ideal plasmas, Ph.D. thesis, Technical University of Eindhoven, Eindhoven, The Netherlands 1987.
[41] H. H. Brouwer and P. P. J. M. Schram, Physica **141A,** 589 (1987).
[42] R. H. Williams and H. E. DeWitt, Phys. Fluids **12,** 2326 (1969).